Desalination and Water Treatment
www.deswater.com
doi: 10.5004/dwt.2019.24574

167 (2019) 313–323
November

Kinetics and characteristics studies on biosorption of Acid Red 18 from aqueous solution by the acid-treated mycelia pellets of *Penicillium janthinellum*

Lifang Zhang*, Fan Wang

School of Environmental and Chemical Engineering, Shenyang Ligong University, Shenyang 110159, China, Tel. +86-15840465862; emails: flz1997@163.com (L. Zhang), ligong_envchem@foxmail.com (F. Wang)

Received 24 February 2019; Accepted 16 June 2019

ABSTRACT

The biosorption of Acid Red 18 from aqueous solutions using nitric acid–treated mycelia pellets of *Penicillium janthinellum* as an adsorbent was studied in a batch system. The effect of solution pH, initial dye concentration, contact time and temperature on biosorption of the dye was carried out. The kinetic data of dye biosorption were analyzed by the pseudo first-order, pseudo second-order, intraparticle diffusion, external diffusion and Boyd models. The nitric acid–treated mycelia pellets of *Penicillium janthinellum* exhibited higher biosorption capacity than the native biomass. The biosorption capacity decreased with increasing pH from 2 to 10 and the maximum biosorption capacity for the dye was 46.45 mg g^{-1} at pH 3 at dye concentration of 50 mg L^{-1}. The dye uptake of the acid-treated biomass increased with increasing the initial dye concentration in the studied concentration range. The kinetic process followed the pseudo second-order with higher correlation coefficients ($R^2 > 0.998$). Based on kinetic models analysis, external diffusion and intraparticle diffusion played important roles in biosorption process and the biosorption rate of the whole biosorption process was mainly controlled by the external diffusion process. The Langmuir isotherm model could well describe the biosorption data. According to the thermodynamic analysis, the biosorption of AR 18 onto the fungal pellets was a spontaneous and endothermic process. The results suggest that the acid-treated mycelia pellets of *Penicillium janthinellum* can be used as an effective biosorbent to remove Acid Red 18 from aqueous solution.

Keywords: Biosorption; *Penicillium janthinellum*; Kinetics; Thermodynamics; Acid Red 18

1. Introduction

Many dyes are used extensively in industrial products such as fabrics, food, carpet, rubber, paper, plastic and cosmetics [1,2]. Most commercial dyes are chemically stable and difficult to be removed from wastewaters [3,4]. The discharge of dye-containing effluents from various industries into aquatic environment adversely affects the natural esthetic quality of water bodies and has a negative impact on aquatic ecosystem by impeding the transmission of sunlight, which can decrease photosynthesis of organisms [5,6]. Furthermore, some synthetic dyes are highly toxic and potentially carcinogenic, mutagenic or allergenic to humans [7–9]. Therefore, it is very important to remove these toxic dyes from the wastewaters before entering the water bodies.

The traditional methods for dye removal include adsorption, biodegradation, photo-catalytic degradation, reverse osmosis, ozonation, flocculation and coagulation. However, those conventional methods are limited by the excessive usage of chemicals, expensive plant requirements or high operational costs [10–13]. It is essential to develop environmentally friendly and highly efficient technologies to remove dyes from wastewater.

* Corresponding author.

In recent decades, more and more focuses have been made on biosorption technology due to its low cost, eco-friendliness and effectiveness. As a promising alternative technology, biosorption is based on non-living microorganisms, plants or agriculture wastes, etc. to remove pollutants such as synthetic dyes, heavy metals and other organic matters from wastewaters [14–16]. The prominent advantages using biomaterials as biosorbents are free of nutrient supply, high selectivity, cost effectiveness and high efficiency [17].

Many microbial organisms including bacteria [18,19], yeast [20], fungus [21,22] and algae [23,24] have been used as biosorbents for dye removal. At present, the biosorbents prepared from microorganisms in single-cell or powdered form, usually have the characteristics of small particle size and low strength, which could increase separation difficulties after adsorption, clogging problems and operation costs. The immobilized microorganisms or other biomaterials by using matrices, such as sodium alginate [20], polyvinyl alcohol [25] and carboxylmethylcellulose (CMC) [26], as supporting materials were also reported to overcome the shortcomings of unimmobilized biomass to remove dyes or heavy metals. However, the immobilization media based on the polymeric gels can increase costs and mass transfer resistance restricting dye diffusion [27]. The use of those biosorbents could be impracticable for the later large-scale application [17,20].

Fungi are filamentous microorganisms, which are widespread in the terrestrial environment. In this study, *Penicillium janthinellum* obtained from the air was used as a biosorbent to remove Acid Red 18(AR 18) from aqueous solution. *Penicillium janthinellum* can form compact mycelia pellets in liquid medium under appropriate growth conditions. The formation of fungal pellets can solve the clogging and afford efficient solid–liquid separation by self-immobilizing without additional supporting materials [22,28]. The mycelia pellets of *Penicillium janthinellum* which have high dye uptake would show promising applications.

The kinetics and mass transfer of biosorption of dye onto the microorganisms with or without the supporting materials have been intensively investigated in recent years, while few literatures were reported on the diffusion and mass transfer kinetics of dye onto the self-immobilizing mycelia pellets. The aim of the present study was to evaluate the characteristics, kinetic mechanism and mass transfer of biosorption of AR 18 from aqueous solution onto the mycelia pellets of *Penicillium janthinellum*. In order to improve the biosorption of AR 18, the mycelia pellets of *Penicillium janthinellum* were treated by 0.1 M nitric acid solution. The biosorption capacity of the nitric acid–treated biomass for AR 18 was explored at different dye concentrations. The various parameters such as pH, initial dye concentration, contact time and temperature were investigated in a batch system. The characteristics of fungal pellets were investigated by SEM, FTIR, zeta potential and alkali titration analysis. The kinetic mechanism in the dye biosorption process was also explored by using the pseudo first-order, pseudo second-order, intraparticle diffusion, external diffusion and Boyd models. The Langmuir and Freundlich isotherm models were used to fit the equilibrium data. The thermodynamics of dye biosorption onto fungal pellets was also investigated.

2. Materials and methods

2.1. Preparation of mycelia pellets of Penicillium janthinellum

The *Penicillium janthinellum* isolated from the air had exhibited the highest dye uptake of AR 18 among the several fungi species, which isolated from the air and soil in earlier study. It was cultivated in liquid medium using the shake flask method. 3 mL (1% inoculation quantity) of spore suspension (3.58×10^7 spores per milliliter distilled water) of *Penicillium janthinellum* was inoculated into 500 mL sterilized conical flask containing 300 mL sterile medium and grew at 150 rpm at 30°C. The growth medium consisted of (g L^{-1} of distilled water): glucose 10, $(NH_4)_2SO_4$ 5, KH_2PO_4 1, $MgSO_4 \cdot 7H_2O$ 0.5. After incubation for 3 d, the mycelia pellets of *Penicillium janthinellum* were harvested from the medium, washed with distilled water several times, then autoclaved at 121°C for 30 min, and stored at 4°C as native biomass.

2 g of native biomass was suspended in 200 mL of 0.1 M HNO_3 and shaken at 120 rpm on a rotary shaker at room temperature for 2 h. After being filtered from the mixture, the biomass was washed several times with distilled water and then stored at 4°C in refrigerator as acid-treated biomass. The moisture content of biomass was determined by drying the desired wet native and acid-treated mycelia pellets in an oven at 65°C for 12 h.

2.2. Biosorption experiments

Acid Red 18 (C.I. 16255, MW 604.48, chemical formula $C_{20}H_{11}N_2O_{10}S_3 \cdot 3Na$ and λ_{max} 505 nm) obtained from Tianjin Tianshun Corporation, China, was used without further purification in this study. The chemical structure of Acid Red 18 is shown in Fig. 1. A stock solution of 1,000 mg L^{-1} of Acid Red 18 (AR 18) was obtained by dissolving 0.5 g of the dye in the 500 mL distilled water. All working solutions in the study were prepared by diluting the dye stock solution with distilled water.

The batch biosorption experiments were investigated by varying pH from 2 to 9, contact time from 0 to 240 min, initial dye concentration from 50 to 500 mg L^{-1} and temperature from 25°C to 40°C with 50 mL AR 18 solution in 150 mL conical flasks in a rotary shaker. The solution pH was adjusted with 0.1 M HCl or NaOH solution. After shaking, the mixture was filtered and the supernatant liquid was analyzed for the remaining dye concentration using a spectrophotometer (721E, Shanghai Spectrum Instrument Co. Ltd., Shanghai, China) at λ_{max} for the dye. All the batch biosorption experiments were carried out in triplicate. The amount of biosorbed dye per unit fungal biomass, q_e (mg g^{-1}), was obtained by using the following expression:

$$q_e = \frac{(C_0 - C_e)V}{m} \tag{1}$$

where q_e is the amount of dye biosorbed onto the unit amount of the biomass (mg g^{-1}). C_0 and C_e represent the concentration of AR 18 in initial solution and after biosorpion (mg L^{-1}), respectively. V is the volume of solution and m is the amount of biosorbent (g, dry weight). The zeta potential measurement of biomass was conducted by using

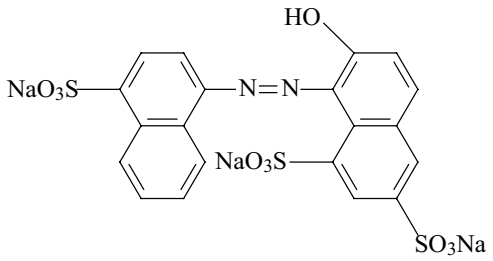

Fig. 1. Chemical structure of Acid Red 18.

zeta potential meter (JS94H2, Shanghai Zhongchen Digital Technique & Equipment Co. Ltd., China).

2.3. Alkali titration experiment

The native and nitric acid–treated biomass samples with wet weight of 0.1 g were suspended in 50 mL distilled water at pH 2 at room temperature, respectively. The mixtures were continuously stirred during the alkali titration experiment with the magnetic stirrer. 0.01 M NaOH solution was added drop by drop into the mixtures and recorded the resulting pH value for each additional 1 mL NaOH solution added.

3. Results and discussion

3.1. Morphology of Penicillium janthinellum

The photo of mycelia pellets of *Penicillium janthinellum* growing for 3 d in the liquid medium is presented in Fig. 2. The figure shows that the mycelia pellets are pale yellowish white with the diameter of about 2–3 mm. The surface morphology of the native and acid-treated mycelia pellets was observed by using the scanning electron micrograph (Fig. 3). As seen from Fig. 3a, it is observed that the mycelia pellet has a network structure composed of fungal mycelia. This network structure means that the mycelia pellet has high specific surface area, which benefits the biosorption of AR 18. In comparison with the native fungal mycelia with even and smooth surface (Fig. 3b), the surface of acid-treated fungal mycelia has rough and uneven surface (Fig. 3c). This may be attributed that nitric acid could remove a slight amount of organic matter from cell wall, leading to inhomogeneous surface of fungal mycelia. The surface property of acid-treated fungal pellets should be considered as a factor providing an increase in the total dye-binding sites.

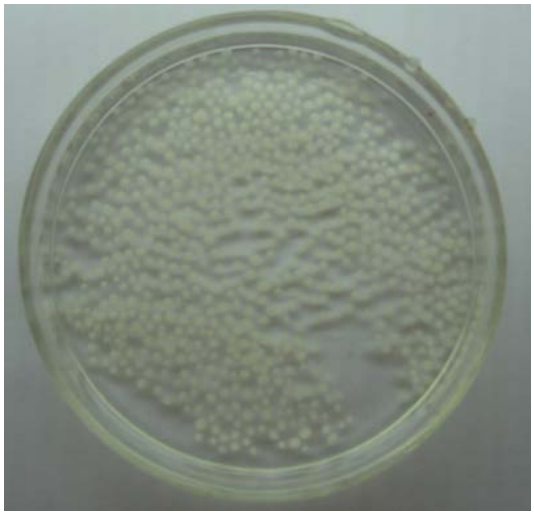

Fig. 2. Photograph of mycelia pellets of *Penicillium janthinellum*.

3.2. FTIR analysis

The cell surface of fungal biomass usually contains polysaccharide, protein and chitin. Those components are composed of varied characteristic functional groups. The FTIR spectra of the mycelium pellets of *Penicillium janthinellum* were carried out to obtain the information of functional groups. It is observed from Fig. 4 that the broad and intense band in the region of 3,500–3,200 cm^{-1} is attributed to N–H asymmetrical stretching vibrations and O–H stretching vibrations. The peaks at 2,928; 2,854; 1,657 and 1,545 cm^{-1} for the biomass are attributed to the symmetric stretching vibration of CH_2, the amide and the amide II, respectively. The adsorption peak in the vicinity of 1,385 cm^{-1} may be distinctive of the amide oscillation as well as the carboxyl group. The vibrational peaks of P = O and P–OH are near at 1,155 and 1,078 cm^{-1}, respectively [29–31]. The results indicate that the mycelium pellets of *Penicillium* sp. contain abundant functional groups such as hydroxyl, carboxyl, amino

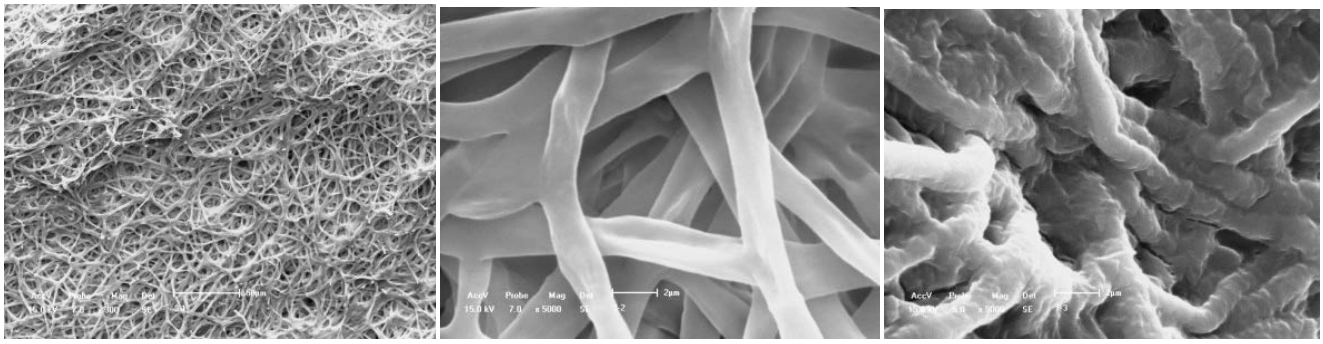

Fig. 3. Scanning electron micrograph of mycelia pellet of *Penicillium janthinellum* (a) native biomass (×300), (b) native biomass (×5,000) and (c) nitric acid-treated biomass (×5,000).

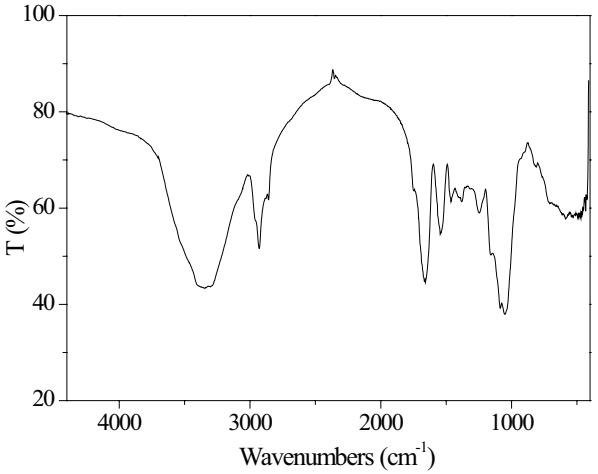

Fig. 4. FTIR spectra of mycelia pellets of *Penicillium janthinellum*.

and phosphate groups, which might be involved in binding AR 18 onto fungal pellets.

3.3. Alkali titration curve analysis

It is important to explore the proton binding active sites of mycelia pellets. Alkali titration plots for the biomass suspensions of the blank (without biomass), native and nitric treated mycelia pellets, respectively, are given in Fig. 5. The alkali titration curves for the three samples show the similar trends with the lower inflection points at pH 2–4 and the upper inflection points at pH 10–12, respectively. As shown in Fig. 5, the values of pH in the systems increased with the increase of the amount of sodium hydroxide added. When the value of pH increased from 2 to 4, the values of sodium hydroxide consumption by the biomass suspensions of the blank, native and acid-treated mycelia pellets were about 3.71, 1.70 and 0.72 mmol, respectively. The values of pH increased sharply to 10 with the increase amount of alkali up to about 1.01 mmol for the blank, 2.09 mmol for the native biomass and 4.07 mmol for acid-treated biomass suspension, respectively, and then the pH slowly increased until the equilibrium trends with further increasing the amount of alkali. It is observed that the values of alkali consumption by the native and acid-treated biomass suspensions at pH 4 and 10 were less than that of the blank, which could be attributed to that the functional groups on surface of fungal pellets could adsorb protons in the systems, resulting in the decreasing consumption of alkali.

The ionization constant pK_H values of functional groups such as amino, carboxyl and phosphoric groups on the surface of the fungal biomass are usually greater than 2 [32]. In strong acid solution, some kind of functional groups could accept protons in the system, leading to the decreased alkali consumption. Fig. 5 also showed that the alkali consumption of the acid-treated biomass suspension was lower than that of the native, suggesting that the adsorption sites on the biomass increased significantly after nitric acid treatment. Therefore, the biosorption capacity of the nitric acid–treated biomass for AR 18 should be higher than that of the native.

3.4. Effect of initial dye concentration

In order to investigate the adsorption capacity of the native and acid-treated mycelia pellets, the effect of initial dye concentration was carried out and the results are presented in Fig. 6. The dye uptake of the native and acid-treated biomass both rapidly increased with increasing the dye concentration from 50 to 300 mg L^{-1} and then increased slowly at dye concentration ranging from 300 to 500 mg L^{-1}. The increase of biosorption capacity with increasing the initial dye concentration is attributed to the increasing driving force to overcome the mass transfer resistances of the dye anions from liquid phases to solid phases. However, all kind of sorbents have a fixed number of adsorption sites, which can reach saturation at a certain adsorbate concentration [14]. Thus, the biosorption of AR 18 onto the fungal pellets showed a saturation trend at higher initial concentration. Meanwhile, the acid-treated fungal biomass had larger biosorption capacity than the native in the dye concentration

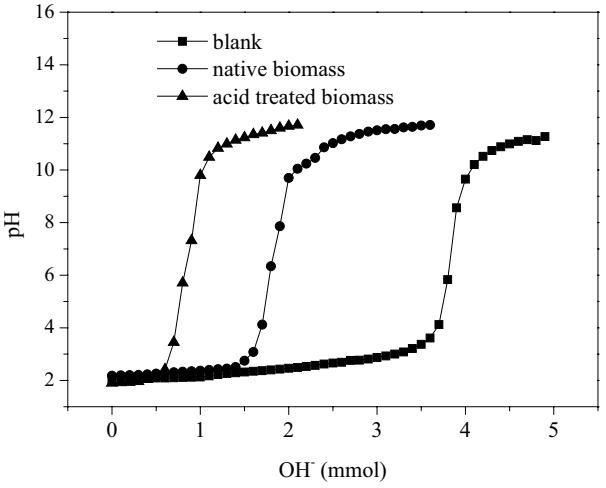

Fig. 5. Alkali titration curves for the native and acid-treated biomass.

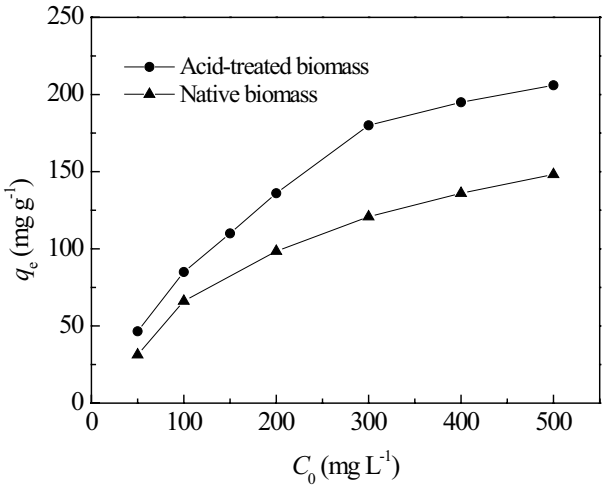

Fig. 6. Effect of initial concentration (biosorbent dosage 0.75 g dry biomass per liter; pH 3; temperature 30°C; contact time 120 min).

range of 50–500 mg L^{-1}. The increased biosorption capacity of acid-treated fungal pellets at all studied dye concentrations can be attributed to the surface modification of biomass by the nitric acid. This further confirms that the acid-treated fungal pellets of *Penicillium janthinellum* gained more new binding sites on the surface.

3.5. Effect of pH

In adsorption process, the initial pH of solution is an important parameter, which affects not only the biosorption capacity but also the ionization of functional groups on the biosorbent [14,16]. Fig. 7 presents the biosorption capacity of the acid-treated biomass for AR 18 as a function of pH. It can be seen that solution pH value has a significant influence on adsorption of the dye by acid-treated biomass. At pH 2–3, the adsorption capacity of acid-treated biomass was higher and the removal rate of the dye reached more than 90%. The adsorption capacity and the removal rate at pH 3 in the studied pH range reached the maximum value, 46.45 mg g^{-1} and 96%, respectively. As dye solution pH increased to 4, the dye uptake of the biomass sharply decreased to only 9.84 mg g^{-1} with a drop of nearly 80% and then the biosorption capacity decreased slightly with the further increase of pH value from 4 to 9. The observation of biosorption of AR 18 at studied pH range could be ascribed to the dissociation of functional groups, such as amino and carboxyl, on the fungal pellets and the AR 18 chemistry. The molecule of AR 18 with azo-based chromophore and three sulfonates can easily dissociate in aqueous solution and release a dye anion and three sodium ions. As the solution pH increased from 2 to 9, the hydroxyl ions also increased, which could compete with the dye anions for the limited binding sites on the fungal pellets, resulting in the decrease in biosorption capacity of the acid-treated fungal pellets [33].

The fungal cell wall is mainly composed of polysaccharide, protein and chitin, which usually contain a large number of functional groups, such as $–NH_2$, –OH, –COOH and $–PO_4$ groups. Those groups can adsorb or release hydrogen ions under certain pH value and protonate or deprotonate. As solution pH changes, thus, the surface functional sites of *Penicillium janthinellum* may be positively or negatively charged by adsorbing or releasing a certain amount of H^+ ions. Zeta potential measurement of the acid-treated *Penicillium janthinellum* was performed in the pH range of 2–10. As seen from Fig. 8, the value of zeta potential of *Penicillium janthinellum* rapidly dropped with an increase of solution pH from 2 to 4. The isoelectric point of the acid-treated biomass is observed at about pH 3.7. Below pH 3.7, the fungal pellets carried net positive charges, which benefited the biosorption of dye anions onto mycelia pellets due to electrostatic attraction between the negatively charged dye anions and the positively charged biosorbent. Above the value, however, the biomass was negatively charged, which inhibited the dye biosorption by electrostatic repulsion between the dye anion and surface of biomass, leading to the decreased biosorption capacity for AR 18 [6,8]. The high biosorption capacity of fungal biomass at pH 2–3 can be explained by the larger electrostatic attraction force due to the high positive charge density on the surface of biomass. The poor biosorption capacity at pH 4–9 may be due to not only the larger electrostatic repulsion caused by the higher negative charge density on the biosorbent but also the competition between hydroxyl ions and dye anions for binding sites on the biomass surface. A rapid decline of biosorption of dye at pH 4 may be partly attributed to strong negative electricity caused by three sulfonates on the dye anion which retard the dye anions toward the negatively charged surface of biomass.

3.6. Biosorption kinetics

The adsorption kinetics process can illustrate the relationship between adsorption material structure and adsorption properties by changing adsorption capacity with time. Fig. 9 shows that biosorption of AR 18 by nitric treated fungal pellets was carried out as a function of contact time at pH 3 and at initial concentration of 50, 100 and 200 mg L^{-1}, respectively. As seen from Fig. 9, the rate of adsorption of dye on the acid-treated biomass increased

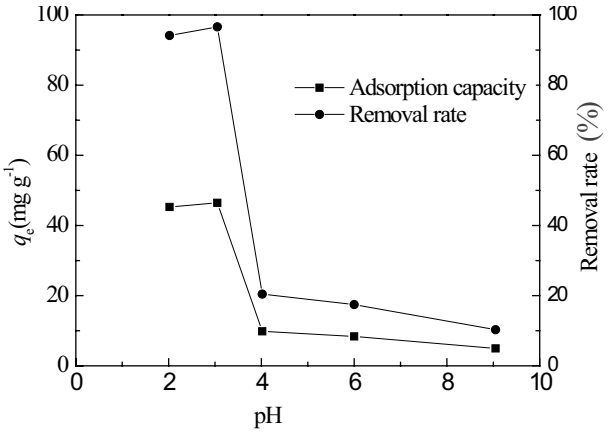

Fig. 7. Effect of pH on biosorption (biosorbent dosage 0.75 g dry biomass per liter; dye concentration 50 mg L^{-1}; temperature 30°C; contact time 120 min).

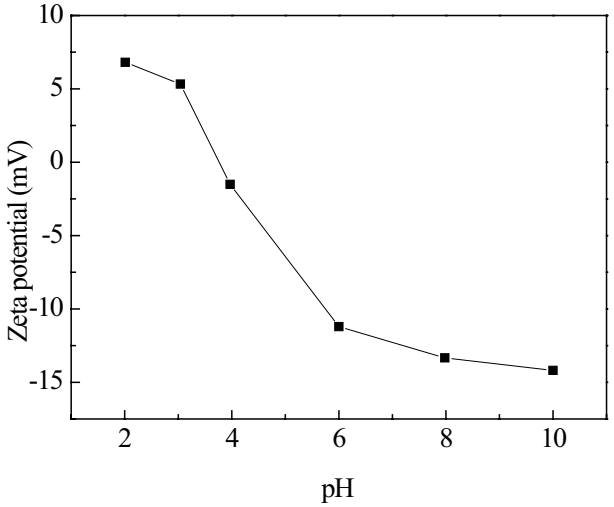

Fig. 8. Zeta potential of acid-treated mycelia pellets of *Penicillium janthinellum*.

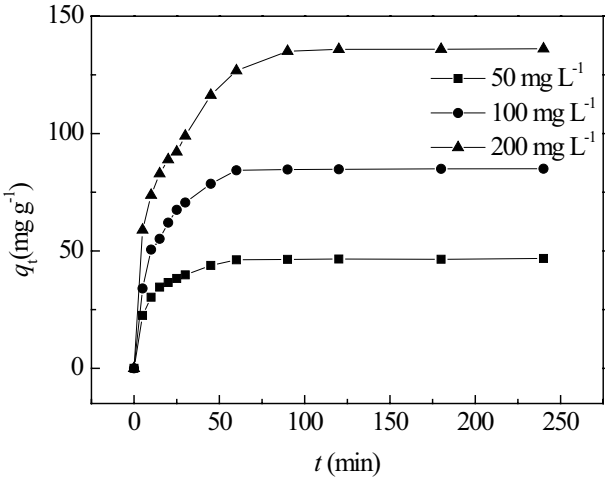

Fig. 9. Effect of time on biosorption (biosorbent dosage 0.75 g dry biomass per liter; pH 3; temperature 30°C).

rapidly within the first 10 min, then slowly deceased with increasing contact time from 10 to 90 min and finally reached the equilibrium at about 60 min for initial dye concentration of 50 and 100 mg L^{-1}, and about 90 min for 200 mg L^{-1}, respectively. The equilibrium time established depended on the initial dye concentration. The decrease of biosorption rate with an increase in contact time may be attributed to the decrease in driving force of dye concentration.

In order to determine the kinetic characteristics and mechanism in the biosorption process, the pseudo first-order, pseudo second-order, intraparticle diffusion, mass transfer and Boyd models were used to analyze the kinetic data in this study.

3.6.1. Pseudo first-order model

The pseudo first-order kinetic model proposed by Lagergren can be expressed as follows [34]:

$$\log(q_e - q_t) = \log q_e - \frac{k_1}{2.303}t \tag{2}$$

where q_e and q_t are the amount of dye adsorbed at equilibrium and at time t (mg g^{-1}) and k_1 is the pseudo first-order adsorption rate constant (min^{-1}). The pseudo first-order kinetic parameters calculated from the slope and intercept of the plots of $\log(q_e - q_t)$ vs. time t at different dye concentrations are presented in Table 1.

As Table 1 shows, the values of linear correlation coefficients (R^2) for pseudo first-order model were in the range of 0.8801–0.9420 and lower than 0.95 at studied dye concentrations. This suggested the pseudo first-order model could not well describe the biosorption data. In addition, the values of calculated equilibrium capacity (q_{cal}), 13.58, 25.60 and 82.15 mg g^{-1} for dye concentration of 50, 100 and 200 mg L^{-1}, respectively, obtained from the equation of pseudo first-order model were obviously lower than the values of experimental equilibrium capacity (q_e), 46.78, 85.03 and 136.44 mg g^{-1} for dye concentration of 50, 100 and 200 mg L^{-1}, respectively. The lower theoretical equilibrium capacities (q_{cal}) further confirms that the biosorption process in the present case does not well follow the pseudo first-order model.

3.6.2. Pseudo second-order model

The pseudo second-order kinetic equation is derived from the adsorption data of divalent metal ions. The specific linear equation can be written as follows [34]:

$$\frac{t}{q_t} = \frac{1}{k_2 q_e^2} + \frac{t}{q_e} \tag{3}$$

where k_2 in the equation is rate constant of pseudo second-order model (g mg^{-1} min^{-1}). The k_2 and q_{cal} can be calculated from the slope and the intercept of the plots of t/q_t vs. t.

The rate constant k_2 does not denote the initial biosorption rate. At $t \to 0$, the initial biosorption rate can be obtained as h_0 (mg min^{-1} g^{-1}) [35]:

$$h_0 = k_2 q_e^2 \tag{4}$$

The theoretical equilibrium capacity (q_{cal}), the initial biosorption rate (h_0), the rate constant k_2 and the correlation coefficient R^2 are given in Table 1. For the pseudo second-order model, the results show the higher correlation coefficients, all greater than 0.99, at all studied concentrations, suggesting that the biosorption of dye onto acid-treated fungal pellets followed the pseudo second-order model more effectively. Meanwhile, the values of theoretical equilibrium capacity, q_{cal} obtained from the linear plots of pseudo second-order kinetic were a lot closer to the experimental q_e values. It is evident that the biosorption of AR 18 onto the acid-treated fungal pellets well obeys the pseudo second-order kinetics, implying that the chemisorption could be involved in the biosorption process [14]. The values of initial biosorption rate (h_0) increased from 6.96 to 14.25 mg min^{-1} g^{-1} as the dye concentration increased from 50 to 200 mg L^{-1},

Table 1
Kinetic parameters for pseudo first-order and pseudo second-order kinetic models

C_0	Pseudo first-order kinetic model				Pseudo second-order kinetic model			
(mg L^{-1})	k_1 (min^{-1})	q_e (mg g^{-1})	q_{cal} (mg g^{-1})	R^2	k_2 (g mg^{-1} min^{-1})	h_0 (mg min^{-1} g^{-1})	q_{cal} (mg g^{-1})	R^2
50	0.0276	46.78	13.58	0.8801	0.00561	6.96	48.08	0.9996
100	0.0385	85.03	25.60	0.9420	0.00164	12.86	88.49	0.9992
200	0.0267	136.44	82.15	0.8745	0.00070	14.25	142.86	0.9986

indicating that the dye concentration in the studied range was significant positive correlation with the initial biosorption rate, that is, the higher studied dye concentration in the studied range increased, the faster the initial adsorption rate became. In addition, Table 1 shows that the values of k_2 decreases with an increase in dye concentration and the theoretical dye uptake. Higher dye uptake indicates that high competition of dye anions onto the limited binding sites of mycelia pellets, resulting in a lower dye diffusion rate [5].

3.6.3. Intraparticle diffusion model

Since the fungal pellets used in the experiment shows a network structure composed of fungal mycelium, it is necessary to analyze the internal diffusion of AR 18 on the mycelia pellets. The intraparticle diffusion of dye adsorption onto biosorbent can be described by Weber–Morris model. The equation can be given as follows [6,7,16]:

$$q_t = k_i t^{0.5} + C \quad (5)$$

where k_i is the dye intraparticle diffusion rate constant (mg g^{-1} min$^{-0.5}$) and C is the constant (mg g^{-1}) and provides an information about the thickness of boundary layer [5,35]. The adsorption dynamics process generally comprises three consecutive steps, including film diffusion, that is, transport of dye molecules from the bulk solution to the external surface of absorbent through the boundary layer diffusion, intraparticle diffusion, that is, diffusion of the dye molecules from the external surface into the adsorbent pores and the dye molecules onto the binding sites of the internal surface of the adsorbent pores [35,36]. The last step is usually faster than the two others and the whole rate of dye adsorption process will be controlled by film diffusion or/and intraparticle diffusion [15]. If the plots gained by Eq. (5) based on adsorption data are straight lines and pass through the origin, it can be concluded that the adsorption process is governed by the intraparticle diffusion. The intraparticle diffusion rate constant, k_i can be obtained from the linear slopes of the plots of q_t vs. $t^{0.5}$.The plots and parameters of the intraparticle diffusion model are given in Fig. 10 and Table 2, respectively.

As shown in Fig. 10, the intraparticle diffusion kinetic plots at all dye concentrations (50, 100, 200 mg L^{-1}) showed multilinearity, comprising of three-stage straight line portions. The first sharper portions within initial 10 min were related to the boundary layer diffusion (film diffusion), suggesting the rapid surface loading. The second straight line portions were attributed to the intraparticle diffusion during the contact time from 10 to 60 min for 50 and 100 mg L^{-1} and from 10 to 90 min for 200 mg L^{-1}, respectively, and the last portions described the final equilibrium stage. The intercept of second-step straight line indicates the thickness of boundary layer. This shows that the larger the value of intercept is, the greater the contribution of the surface sorption in the rate-controlling step is [5,30]. The value of intercept of the second portion increased from 21.01 to 43.17 mg g^{-1} (Table 2) with increasing dye concentration from 50 to 100 mg L^{-1}, indicating that the boundary layer effect was not negligible during the biosorption of AR 18 onto the acid-treated fungal pellets. The greater the value of intraparticle diffusion rate k_i, the faster the adsorbate diffuses from the external surface into the adsorbent pores. The increase of k_i value from the second portion intraparticle diffusion with increasing AR 18 concentration suggested that the dye anions easily diffused from the surface of fungal pellets to the interior under higher initial dye concentration. It is attributed to the reason that the increase of dye concentration results in an increase of the driving force, which can increase the diffusion rate of AR 18. Thus, the higher initial dye concentration provides the higher diffusion coefficient, resulting in higher biosorption capacity for AR 18. The multi-stage plots mean that the intraparticle diffusion is not only limiting step in the dye biosorption process.

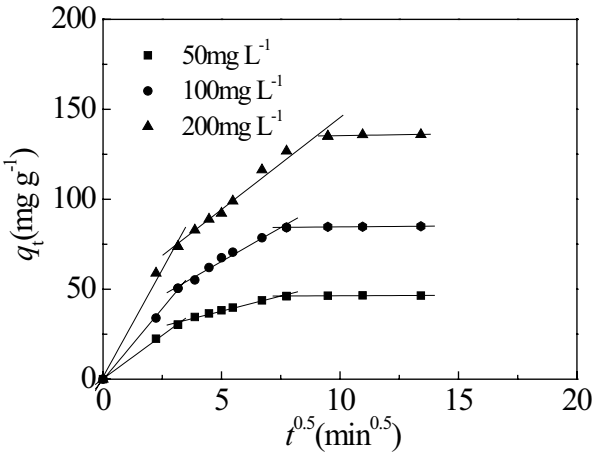

Fig. 10. Intraparticle diffusion kinetic model for dye biosorption.

3.6.4. External diffusion model

According to the adsorption theory, in most cases, the adsorption rate is mainly controlled by the external diffusion process or the intraparticle diffusion process or both.

Table 2
Parameters obtained from the intraparticle and the external diffusion models

	Intraparticle diffusion			External diffusion	
C_0 (mg L^{-1})	k_i (mg g^{-1} min$^{-0.5}$)	C (mg g^{-1})	R^2	$\beta_L S$ (min^{-1})	R^2
50	3.35	21.04	0.9797	0.0339	0.9871
100	7.533	27.67	0.9835	0.0248	0.9777
200	10.23	43.17	0.9779	0.0092	0.9515

The diffusion coefficient of external diffusion can be obtained by Mathews–Weber model. The Mathews–Weber model is expressed as [26,37,38]:

$$\frac{C_t}{C_0} = e^{-\beta_L S_t} \tag{6}$$

where C_t is the dye concentration at time t, C_0 is the initial dye concentration, β_L is the mass transfer coefficient, and S is the external surface area of the adsorbent. Since the S value in the model is difficult to determine, the rate of mass transfer of external diffusion is estimated by the value of $\beta_L S$ in the adsorption process.

The external diffusion curves can be obtained by plotting C_t/C_0 vs. t at different dye concentrations (Fig. 11). As shown in Fig. 11, C_t/C_0 decreased with the increase of contact time until biosorption equilibrium and increased with the increase of the initial dye concentration. The values of $\beta_L S$ calculated from the slope of linear plots of ln (C_t/C_0) against time t are presented in Table 2. When the initial dye concentration increased from 50 to 200 mg L^{-1}, the $\beta_L S$ value decreased from 0.0339 to 0.0092 min^{-1}. It is indicated that the higher the dye concentration, the slower the mass transfer rate of dye from liquid to solid phase is. The decrease of $\beta_L S$ value with the increase in the initial AR 18 concentration may be due to the increase in boundary layer thickness (C), which is obtained from the intercept of the second straight portion in intraparticle diffusion plot. The results are also in agreement with k_2 obtained from pseudo second-order kinetic equation. However, the increasing dye concentration does favor the intraparticle diffusion of AR 18. The larger $\beta_L S$ values for the dye concentration of 50 and 100 mg L^{-1} result in equilibrium faster for biosorption of AR 18 onto fungal pellets.

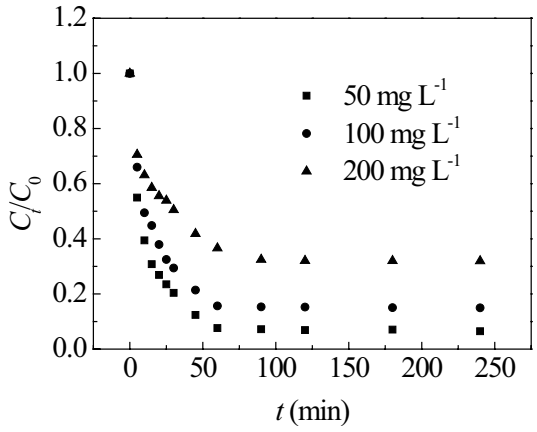

Fig. 11. Plots of C_t/C_0- t at different initial dye concentrations.

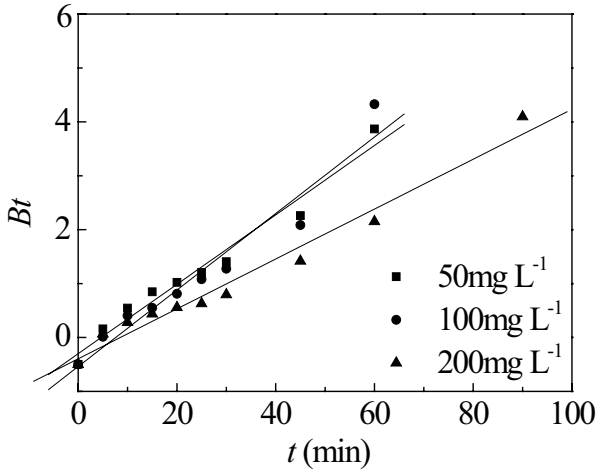

Fig. 12. Boyd plots of biosorption.

3.6.5. Boyd model

The Boyd model is usually used to determine the rate control step of the adsorption process, and its expression can be given as [39,40] follows:

$$\mathrm{Bt} = -0.498 - \ln(1 - F) \tag{7}$$

$$F = \frac{q_t}{q_e} \tag{8}$$

where F is the biosorption separation coefficient at time t and Bt is a function of F.

It is generally believed that if the plot of Bt vs. t shows a good linearity and passes through the origin, the intraparticle diffusion is the rate limiting step of dye biosorption, otherwise the film diffusion is the rate limiting step [39]. In order to further determine the rate limiting step of dye biosorption, Boyd model plots are shown in Fig. 12. The plots for dye concentration of 50 and 100 mg L^{-1} showed good linearity, but did not pass through the origin. While the concentration of dye was 200 mg L^{-1}, the linearity of the plot was poor and the plot also did not pass through the origin. This indicated that the film diffusion process was mainly rate limiting step for AR 18 biosorption onto acid-treated fungal pellets. The similar results were reported for basic Violet 3 and Acid Black 1 adsorption onto unburned carbon [39], the basic yellow dye onto green alga *Caulerpa scalpelliformis* [41], and the hexavalent chromium by dead fungal biomass of marine *Aspergillus niger* [40], respectively.

3.7. Biosorption isotherms

The equilibrium adsorption isotherm is fundamentally important in the practical design of adsorption systems [42]. Adsorption isotherms also can describe the relationship between the adsorbate and sorbent [5]. In this study, biosorption isotherms were investigated at different temperatures (25°C–40°C) by varying the initial concentration of AR 18 from 50 to 500 mg L^{-1}. The Langmuir and Freundlich isotherm models were used to fit the equilibrium adsorption data at 25°C, 30°C, 35°C and 40°C.

The linear equation of the Langmuir and Freundlich isotherm models, respectively, is given by [5,15]:

$$\frac{C_e}{q_e} = \frac{C_e}{q_m} + \frac{1}{b \times q_m} \tag{9}$$

$$\log q_e = \left(\frac{1}{n}\right) \log C_e + \log K_F \quad (10)$$

where C_e is concentration of dye at equilibrium (mg L^{-1}), b is Langmuir constant (L mg^{-1}), q_m is the monolayer adsorption capacity (mg g^{-1}) and q_e represents amounts of dye adsorbed on biosorbent at equilibrium (mg g^{-1}). K_F and n are indicative isotherm parameters of adsorption capacity and intensity, respectively. The Langmuir and Freundlich constants can be determined from slope and intercept of the linear plots of C_e/q_e vs. C_e (Fig. 13) and log q_e vs. log C_e (Fig. 14), respectively. The parameters of both isotherm models are given in Table 3. The values of correlation coefficients (R^2) for Langmuir isotherm model were found to be all greater than 0.98 at temperature ranging from 25°C to 40°C, respectively. The higher correlation coefficients at studied temperature showed that the biosorption of AR 18 onto the acid-treated mycelium pellets of *Penicillium janthinellum* followed the Langmuir better than the Freundlich isotherm model. The values of 1/n were all between 0 and 1, suggesting that the biosorption of AR 18 onto the acid-treated mycelia pellets is favorable at studied temperature range [6,43,44]. Furthermore, the maximum adsorption capacities (q_m) of the acid-treated biomass were determined as 250.0, 312.5, 333.3 and 357.1 mg g^{-1} at 25°C, 30°C, 35°C and 40°C, respectively. An increase in the equilibrium monolayer capacity with increasing the temperature from 25°C to 40°C shows that the biosorption process was endothermic in the studied temperature range.

3.8. Thermodynamic analysis

The temperature-dependent biosorption process is associated with thermodynamic parameters, which reflect the feasibility and spontaneous nature of the biosorption process [15]. The Gibbs free energy change (ΔG°), enthalpy (ΔH°) and entropy (ΔS°) can be determined from the following equations [8,45]:

$$\Delta G° = -RT \ln K_D \quad (11)$$

$$\ln K_D = \frac{\Delta S°}{R} - \frac{\Delta H°}{RT} \quad (12)$$

where K_D is the distribution constant and T is absolute temperature. The values of ΔG°, ΔH° and ΔS° for the biosorption of AR 18 onto the acid-treated *Penicillium janthinellum* at different temperatures are presented in Table 4. The negative values of ΔG° indicated the biosorption of AR 18 was a spontaneous in nature at different temperatures (25°C–40°C). The value of enthalpy change was positive, suggesting the adsorption process was endothermic. The adsorption capacity increased with a rise in temperature. The positive value of ΔS° suggested increasing randomness at the solid–liquid interface during the biosorption of AR 18 onto acid-treated *Penicillium janthinellum*.

Table 3
Langmuir and Freundlich isotherm parameters for biosorption of AR 18

	Langmuir isotherm			Freundlich isotherm		
T (°C)	R^2	q_0 (mg g^{-1})	B (L mg^{-1})	R^2	K_F	1/n
25	0.992	250.0	0.0124	0.984	14.4	0.469
30	0.984	312.5	0.0137	0.993	16.0	0.506
35	0.997	333.3	0.0199	0.960	24.8	0.451
40	0.998	357.1	0.0273	0.930	33.3	0.426

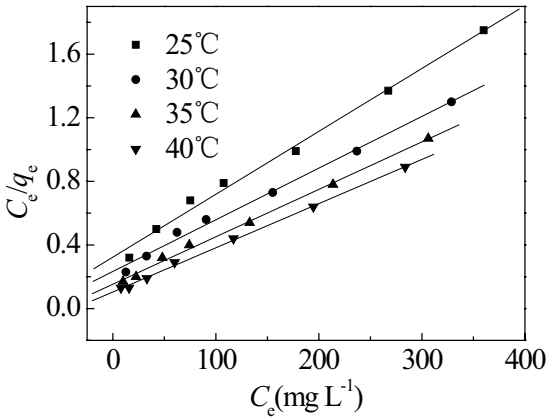

Fig. 13. Linear plots of Langmuir isotherm for biosorption of AR 18 (biosorbent dosage 0.75 g dry biomass per liter; pH 3; contact time 120 min).

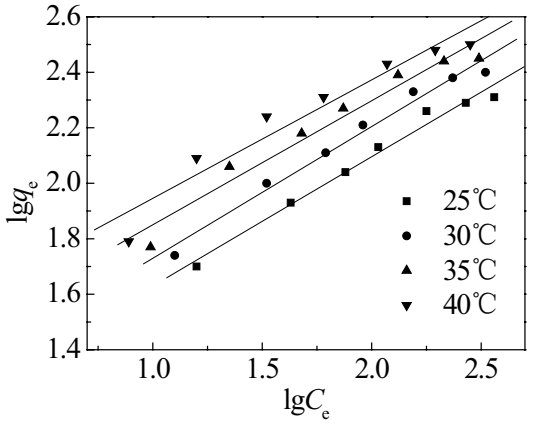

Fig. 14. Linear plots of Freundlich isotherm for biosorption of AR 18 (biosorbent dosage 0.75 g dry biomass per liter; pH 3; contact time 120 min).

Table 4
Thermodynamic parameters for biosorption of AR 18

T (°C)	ΔG (kJ mol^{-1})	ΔS (J mol^{-1} K^{-1})	ΔH (kJ mol^{-1})
25	–1.10	109.45	31.53
30	–1.59		
35	–2.21		
40	–2.72		

4. Conclusion

The mycelia pellets of *Penicillium janthinellum* treated with nitric acid had higher adsorption capacity for AR 18 than the native. Based on the alkali titration curves analysis, it was indicated that the nitric acid treatment could increase the new active site on the biomass. The biosorption process followed pseudo second-order kinetic model with higher correlation coefficient. According to the kinetic analysis, the external diffusion and intraparticle diffusion were involved in the dye biosorpton process. The biosorption rate of the whole adsorption process was mainly controlled by the external diffusion process. The biosorption of AR 18 followed the Langmuir better than the Freundlich isotherm model. The thermodynamic analysis suggested that the biosorption process was spontaneous and endothermic in nature.

References

[1] F.C. Wu, R.L. Tseng, High adsorption capacity NaOH-activated carbon for dye removal from aqueous solution, J. Hazard. Mater., 152 (2008) 1256–1267.

[2] P.T. Juchen, H.H. Piffer, M.T. Veit, G.d.C. Gonçalves, S.M. Palácio, J.C. Zanette, Biosorption of reactive blue BF-5G dye by malt bagasse: kinetic and equilibrium studies, J. Environ. Chem. Eng., 6 (2018) 7111–7118.

[3] M.E. Fernandez, G.V. Nunell, P.R. Bonelli, A.L. Cukierman, Batch and dynamic biosorption of basic dyes from binary solutions by alkaline-treated cypress cone chips, Bioresour. Technol., 106 (2012) 55–62.

[4] N. El Messaoudi, M. El Khomri, A. Dbik, S. Bentahar, A. Lacherai, B. Bakiz, Biosorption of Congo red in a fixed-bed column from aqueous solution using jujube shell: experimental and mathematical modeling, J. Environ. Chem. Eng., 4 (2016) 3848–3855.

[5] R. Kumar, R. Ahmad, Biosorption of hazardous crystal violet dye from aqueous solution onto treated ginger waste (TGW), Desalination, 265 (2011) 112–118.

[6] Y. Yang, G. Wang, B. Wang, Z. Li, X. Jia, Q. Zhou, Y. Zhao, Biosorption of Acid Black 172 and Congo Red from aqueous solution by nonviable Penicillium YW 01: kinetic study, equilibrium isotherm and artificial neural network modeling, Bioresour. Technol., 102 (2011) 828–834.

[7] T. Akar, S. Celik, S.T. Akar, Biosorption performance of surface modified biomass obtained from *Pyracantha coccinea* for the decolorization of dye contaminated solutions, Chem. Eng. J., 160 (2010) 466–472.

[8] N. Barka, M. Abdennouri, M. EL Makhfouk, Removal of Methylene Blue and Eriochrome Black T from aqueous solutions by biosorption on *Scolymus hispanicus* L.: kinetics, equilibrium and thermodynamics, J. Taiwan Inst. Chem. Eng., 42 (2011) 320–326.

[9] X.J. Xiong, X.J. Meng, T.L. Zheng, Biosorption of C.I. Direct Blue 199 from aqueous solution by nonviable *Aspergillus niger*, J. Hazard. Mater., 175 (2010) 241–246.

[10] R. Dallel, A. Kesraoui, M. Seffen, Biosorption of cationic dye onto "*Phragmites australis*" fibers: characterization and mechanism, J. Environ. Chem. Eng., 6 (2018) 7247–7256.

[11] Y.A.R. Lebron, V.R. Moreira, L.V.S. Santos, R.S. Jacob, Remediation of methylene blue from aqueous solution by *Chlorella pyrenoidosa* and *Spirulina maxima* biosorption: equilibrium, kinetics, thermodynamics and optimization studies, J. Environ. Chem. Eng., 6 (2018) 6680–6690.

[12] J. Huang, D. Liu, J. Lu, H. Wang, X. Wei, J. Liu, Biosorption of reactive black 5 by modified *Aspergillus versicolor* biomass: kinetics, capacity and mechanism studies, Colloids. Surf., A, 492 (2016) 242–248.

[13] S. Bera, V.P. Sharma, S. Dutta, D. Dutta, Biological decolorization and detoxification of malachite green from aqueous solution by *Dietzia maris* NIT-D, J. Taiwan Inst. Chem. Eng., 67 (2016) 271–284.

[14] S. Chowdhury, S. Chakraborty, P. Saha, Biosorption of Basic Green 4 from aqueous solution by *Ananas comosus* (pineapple) leaf powder, Colloids. Surf., B, 84 (2011) 520–527.

[15] F. Deniz, S.D. Saygideger, Equilibrium, kinetic and thermodynamic studies of Acid Orange 52 dye biosorption by *Paulownia tomentosa* Steud. leaf powder as a low-cost natural biosorbent, Bioresour. Technol., 101 (2010) 5137–5143.

[16] T. Akar, M. Divriklioglu, Biosorption applications of modified fungal biomass for decolorization of Reactive Red 2 contaminated solutions: batch and dynamic flow mode studies, Bioresour. Technol., 101 (2010) 7271–7277.

[17] J. Mao, S. W. Won, K. Vijayaraghavan, Y.S. Yun, Immobilized citric acid-treated bacterial biosorbents for the removal of cationic pollutants, Chem. Eng. J., 162 (2010) 662–668.

[18] J. Mao, I.S. Kwak, M. Sathishkumar, K. Sneha, Y.S. Yun, Preparation of PEI-coated bacterial biosorbent in water solution: optimization of manufacturing conditions using response surface methodology, Bioresour. Technol., 102 (2011) 1462–1467.

[19] S.Y. Kim, M.R. Jin, C.H. Chung, Y.S. Yun, K.Y. Jahng, K.Y. Yu, Biosorption of cationic basic dye and cadmium by the novel biosorbent *Bacillus catenulatus* JB-022 strain, J. Biosci. Bioeng., 119 (2015) 433–439.

[20] D. Charumathi, N. Das, Packed bed column studies for the removal of synthetic dyes from textile wastewater using immobilised dead *C. tropicalis*, Desalination, 285 (2012) 22–30.

[21] M.S. Mahmoud, M.K. Mostafa, S.A. Mohamed, N.A. Sobhy, M. Nasr, Bioremediation of red azo dye from aqueous solutions by *Aspergillus niger* strain isolated from textile wastewater, J. Environ. Chem. Eng., 5 (2017) 547–554.

[22] M.X. Wang, Q.L. Zhang, S.J. Yao, A novel biosorbent formed of marine-derived *Penicillium janthinellum* mycelial pellets for removing dyes from dye-containing wastewater, Chem. Eng. J., 259 (2015) 837–844.

[23] M. Kousha, E. Daneshvar, H. Dopeikar, D. Taghavi, A. Bhatnagar, Box–Behnken design optimization of Acid Black 1 dye biosorption by different brown macroalgae, Chem. Eng. J., 179 (2012) 158–168.

[24] E. Daneshvar, A. Vazirzadeh, A. Niazi, M. Sillanpää, A. Bhatnagar, A comparative study of methylene blue biosorption using different modified brown, red and green macroalgae – effect of pretreatment, Chem. Eng. J., 307 (2017) 435–446.

[25] W.C. Kao, J.Y. Wu, C.C. Chang, J.S. Chang, Cadmium biosorption by polyvinyl alcohol immobilized recombinant *Escherichia coli*, J. Hazard. Mater., 169 (2009) 651–658.

[26] B.E. Wang, Y.Y. Hu, L. Xie, K. Peng, Biosorption behavior of azo dye by inactive CMC immobilized *Aspergillus fumigatus* beads, Bioresour. Technol., 99 (2008) 794–800.

[27] A. Saeed, M. Iqbal, S.I. Zafar, Immobilization of *Trichoderma viride* for enhanced methylene blue biosorption: batch and column studies, J. Hazard. Mater., 168 (2009) 406–415.

[28] V.K. Gupta Suhas, Application of low-cost adsorbents for dye removal: a review, J. Environ. Manage., 90 (2009) 2313–2342.

[29] S. Özdemir, E. Kilinc, A. Poli, B. Nicolaus, K. Güven, Biosorption of Cd, Cu, Ni, Mn and Zn from aqueous solutions by thermophilic bacteria, *Geobacillus toebii* sub. sp. *decanicus* and *Geobacillus thermoleovorans* sub. sp. *stromboliensis*: equilibrium, kinetic and thermodynamic studies, Chem. Eng. J., 152 (2009) 195–206.

[30] A. Sari, D. Mendil, M. Tuzen, M. Soylak, Biosorption of Cd(II) and Cr(III) from aqueous solution by moss (*Hylocomium splendens*) biomass: equilibrium, kinetic and thermodynamic studies, Chem. Eng. J., 144 (2008) 1–9.

[31] J. Ye, H. Yin, B. Mai, H. Peng, H. Qin, B. He, N. Zhang, Biosorption of chromium from aqueous solution and electroplating wastewater using mixture of *Candida lipolytica* and dewatered sewage sludge, Bioresour. Technol., 101 (2010) 3893–3902.

[32] Y. Tian, C. Ji, M. Zhao, M. Xu, Y. Zhang, R. Wang, Preparation and characterization of baker's yeast modified by nano-Fe_3O_4: application of biosorption of methyl violet in aqueous solution, Chem. Eng. J., 165 (2010) 474–481.

[33] O. Aksakal, H. Ucun, Equilibrium, kinetic and thermodynamic studies of the biosorption of textile dye (Reactive Red 195) onto *Pinus sylvestris* L., J. Hazard. Mater., 181 (2010) 666–672.
[34] A. Robalds, L. Dreijalte, O. Bikovens, M. Klavins, A novel peat-based biosorbent for the removal of phosphate from synthetic and real wastewater and possible utilization of spent sorbent in land application, Desal. Wat. Treat., 57 (2016) 13285–13294.
[35] M.I. El-Khaiary, Kinetics and mechanism of adsorption of methylene blue from aqueous solution by nitric-acid treated water-hyacinth, J. Hazard. Mater., 147 (2007) 28–36.
[36] G.L. Dotto, L.A.A. Pinto, Analysis of mass transfer kinetics in the biosorption of synthetic dyes onto *Spirulina platensis* nanoparticles, Biochem. Eng. J., 68 (2012) 85–90.
[37] L. Khezami, R. Capart, Removal of chromium(VI) from aqueous solution by activated carbons: kinetic and equilibrium studies, J. Hazard. Mater., B123 (2005) 223–231.
[38] A. Özer, G. Akkayaa, M. Turabik, The biosorption of Acid Red 337 and Acid Blue 324 on *Enteromorpha prolifera*: the application of nonlinear regression analysis to dye biosorption, Chem. Eng. J., 112 (2005) 181–190.
[39] S. Wang, H. Li, Kinetic modelling and mechanism of dye adsorption on unburned carbon, Dyes Pigm., 72 (2007) 308–314.
[40] Y. Khambhaty, K. Mody, S. Basha, B. Jha, Kinetics, equilibrium and thermodynamic studies on biosorption of hexavalent chromium by dead fungal biomass of marine *Aspergillus niger*, Chem. Eng. J., 145 (2009) 489–495.
[41] R. Aravindhan, J. Raghava Rao, B.U. Nair, Removal of basic yellow dye from aqueous solution by sorption on green alga *Caulerpa scalpelliformis*, J. Hazard. Mater., 142 (2007) 68–76.
[42] A. Özer, G. Akkaya, M. Turabik, Biosorption of Acid Red 274 (AR 274) on *Enteromorpha prolifera* in a batch system, J. Hazard. Mater., B126 (2005) 119–127.
[43] C. Kannan, N. Buvaneswari, T. Palvannan, Removal of plant poisoning dyes by adsorption on tomato plant root and green carbon from aqueous solution and its recovery, Desalination, 249 (2009) 1132–1138.
[44] B.H. Hameed, A.A. Ahmad, N. Aziz, Isotherms, kinetics and thermodynamics of acid dye adsorption on activated palm ash, Chem. Eng. J., 133 (2007) 195–203.
[45] C.P.J. Isaac, A. Sivakumar, Removal of lead and cadmium ions from water using *Annona squamosa* shell: kinetic and equilibrium studies, Desal. Wat. Treat., 51 (2013) 7700–7709.